Article

Cell Reports

Cdx and T Brachyury Co-activate Growth Signaling in the Embryonic Axial Progenitor Niche

Graphical Abstract

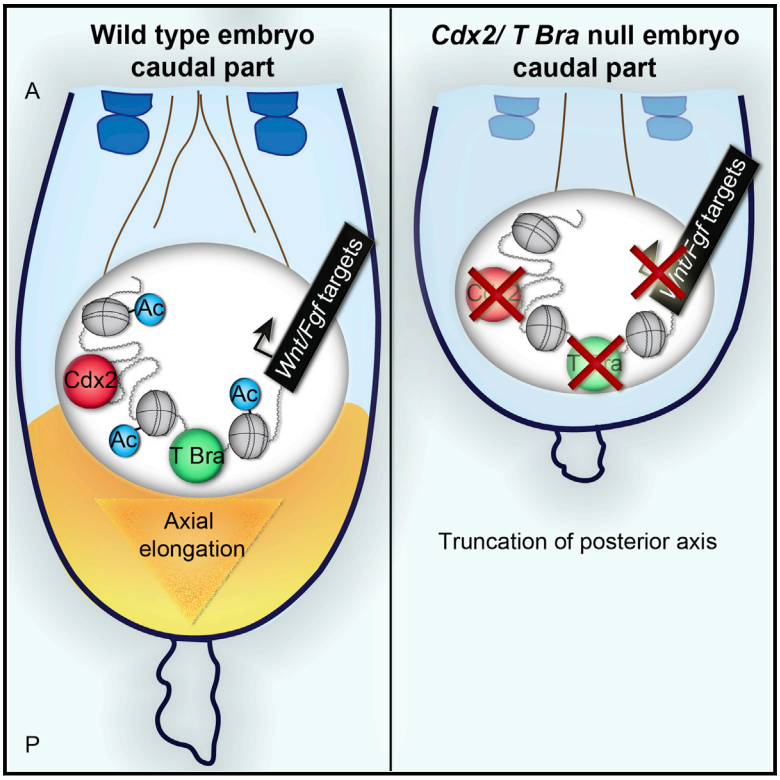

Authors

Shilu Amin, Roel Neijts, Salvatore Simmini, ..., Alexander van Oudenaarden, Menno P. Creyghton, Jacqueline Deschamps

Correspondence

j.deschamps@hubrecht.eu

In Brief

Vertebrate embryos elongate their body from a posterior growth zone containing tissue progenitors. Amin et al. find that two different transcription factors required for body elongation directly bind and activate the same growth-stimulating genes. The authors demonstrate the importance of these activation events for differential control of axial growth.

Highlights

- Expression of *Cdx2* is essential for posterior neuro-mesodermal axial progenitors
- *Cdx2/T Brachyury* double mutants are more severely truncated than single mutants
- Cdx2 and T Brachyury directly co-activate genes of the Wnt and Fgf signaling pathways
- The genetic network driven by Cdx/Hox and *T Brachyury* establishes differential axial growth

Accession Numbers

GSE84899
GSE81203

Amin et al., 2016, Cell Reports *17*, 3165–3177
December 20, 2016
http://dx.doi.org/10.1016/j.celrep.2016.11.069

Cell Reports
Article

Cdx and T Brachyury Co-activate Growth Signaling in the Embryonic Axial Progenitor Niche

Shilu Amin,[1,2] Roel Neijts,[1,2] Salvatore Simmini,[1] Carina van Rooijen,[1] Sander C. Tan,[1] Lennart Kester,[1] Alexander van Oudenaarden,[1] Menno P. Creyghton,[1] and Jacqueline Deschamps[1,3,*]
[1]Hubrecht Institute and UMC Utrecht, Uppsalalaan 8, 3584 CT Utrecht, the Netherlands
[2]Co-first author
[3]Lead Contact
*Correspondence: j.deschamps@hubrecht.eu
http://dx.doi.org/10.1016/j.celrep.2016.11.069

SUMMARY

In vertebrate embryos, anterior tissues are generated early, followed by the other axial structures that emerge sequentially from a posterior growth zone. The genetic network driving posterior axial elongation in mice, and its disturbance in mutants with posterior truncation, is not yet fully understood. Here, we show that the combined expression of *Cdx2* and *T Brachyury* is essential to establish the core signature of posterior axial progenitors. *Cdx2* and *T Brachyury* are required for extension of a similar trunk portion of the axis. Simultaneous loss of function of these two genes disrupts axial elongation to a much greater extent than each single mutation alone. We identify and validate common targets for Cdx2 and T Brachyury in vivo, including Wnt and Fgf pathway components active in the axial progenitor niche. Our data demonstrate that integration of the Cdx/Hox and T Brachyury transcriptional networks controls differential axial growth during vertebrate trunk elongation.

INTRODUCTION

Our understanding of early post-implantation mouse development has increased considerably in recent years, thanks to the refinement of new molecular genetic approaches and the accumulation of morphogenetic information (Rivera-Pérez and Hadjantonakis, 2014). This is true in particular for the anterior-to-posterior growth of embryonic tissues in the three germ layers. The genetic regulation of posterior axial elongation is an evolutionarily conserved process in bilaterian animals (Martin and Kimelman, 2009; Neijts et al., 2014). In the mouse, progenitors that supply cells for the different axial tissues of the trunk and tail during the sequential laying down of the anteroposterior (AP) structures are present along the primitive streak. Some of these progenitors are generating mesoderm exclusively, whereas a particular population residing in the anteriormost part of the streak represents bipotent neuromesodermal progenitors (NMPs) that retain the capacity to generate both neural and mesodermal lineages (Cambray and Wilson, 2002, 2007; Tzouanacou et al., 2009; Wymeersch et al., 2016). NMPs have received considerable attention, as they possess self-renewing properties (Gouti et al., 2014; Tsakiridis et al., 2014; Turner et al., 2014) and are a key cell population that drives the successive steps of axial tissue generation.

Cdx genes are known to be involved in axial elongation, because their inactivation in mice gave rise to embryos with a shortened axis (Chawengsaksophak et al., 1997; van den Akker et al., 2002). All three Cdx genes contribute to this function, the most potent being *Cdx2* (Chawengsaksophak et al., 2004; van Rooijen et al., 2012). Cdx genes are expressed early in the primitive streak and later in the tail bud, where they are required for growth of posterior embryonic tissues until the axis is fully extended. Mutants totally missing active Cdx genes develop anterior structures normally but fail to generate any post-occipital tissue (van Rooijen et al., 2012). *Cdx2* null mutants are impaired in generating their axis posteriorly to somite 7 to 12. Inactivation of *Cdx1* and/or *Cdx4* does not alter axial elongation, but the truncation phenotype of *Cdx2* null mutants is more severe in combination with the inactivation of one of the other two Cdx genes. Rescue experiments in vivo (Young et al., 2009) and in embryos in culture (van Rooijen et al., 2012) have indicated that Cdx genes act in axial elongation at least in part by maintaining Wnt and Fgf signaling active in the posterior growth zone, suggesting that these may represent key downstream targets for Cdx transcriptional activity.

In addition to Cdx, another transcription factor required for complete posterior axis elongation is T Brachyury (T Bra). *T Bra* is expressed in the primitive streak and early mesoderm at gastrulation stages, and in the growth zone of the tail bud subsequently until around embryonic day (E)14.5 (Wilkinson et al., 1990). Similar to *Cdx2* null mutants, *T Bra* null embryos generate about seven somites, after which axis elongation is impaired. In addition, the neural tube is kinked in its posterior portion and abnormal somites are observed. This is likely due to the fact that T Bra plays a role in mesoderm specification as well as in somitogenesis (Martin, 2016; Wilson and Beddington, 1997). We now show that the null mutations in *Cdx2* and *T Bra* synergize in their effects on embryonic axial elongation. We aimed at investigating whether this synergism, added to the similarity between the posterior truncation phenotypes of *Cdx2* and *T Bra* mutants, results from the same molecular mechanism of action. Similar to the situation for Cdx2, *T Bra* regulates the Wnt signaling pathway

(Martin and Kimelman, 2008) and the Fgf pathway, as *Fgf8* was identified as a target of T Bra in differentiating mouse embryonic stem cells (Lolas et al., 2014).

Recent work demonstrated that the co-expression of *T Bra* and the stem cell marker *Sox2* is linked to a core transcriptional signature in these NMPs (Olivera-Martinez et al., 2012; Wymeersch et al., 2016). T Bra is required for the activity of the axial progenitors contributing descendants at axial levels posterior to somite 7, the region described above to be dependent on Cdx2 for its generation. In order to understand whether Cdx2, like T Bra, maintains the axial progenitor niche proficient, and how this is executed by these transcription factors, we set out to determine and compare the downstream programs of both Cdx2 and T Bra during posterior axis elongation. We used a homogeneous ex vivo system based on pre-gastrulation embryo-derived epiblast stem cells (EpiSCs) as a model for the posterior growth zone of the embryo. When induced with Wnt and Fgf, these cells closely represent the primitive streak epiblast, including the NMPs described above (Tsakiridis et al., 2014; Tsakiridis and Wilson, 2015). We performed genome-wide binding analysis for direct targets of Cdx2 and T Bra in these cells by chromatin immunoprecipitation with massively parallel sequencing (ChIP-seq). We identified an overlapping set of target genes, including members of the Fgf and Wnt signaling cascades. We validated the Cdx/T Bra-binding regions as transcriptional enhancers of the target genes using *lacZ* reporter assays. We propose that *Cdx2* expression participates in the core signature of NMPs and conclude that Cdx2 and T Bra stimulate axial extension by directly co-activating the Wnt and Fgf growth signaling cascades, both at the level of the axial progenitors themselves and at the level of their niche.

RESULTS

Epiblast Stem Cells Are a Valid Model of Posterior Embryonic Elongation

Posterior elongation of the axis to generate the trunk and tail tissues occurs from cell progenitors in the primitive streak region in the posterior part of the mouse embryo between the late streak and early somite stages and around E14.5. Several transcription factors and signaling pathways are known to be instrumental in this process, as shown by the posterior truncation phenotype resulting from their invalidation in mutants. This is the case for T Bra (Herrmann et al., 1990) and Cdx2 (Chawengsaksophak et al., 2004) and genes of the Wnt (Galceran et al., 1999; Takada et al., 1994) and Fgf (Hoch and Soriano, 2006; Naiche et al., 2011) pathways.

To study these processes, we used a model for posterior axis elongation. EpiSCs can be directed toward a primitive streak-like fate by Wnt3a (or the Wnt agonist CHIR99021; Chiron) and Fgf. A proportion of these cells qualify as NMPs that contribute descendants to the elongating trunk and tail tissues (Tsakiridis et al., 2014) (Figure 1A). Induced EpiSCs exhibit specific features of axial stem cells, as shown by the increased availability of the *Sox2 N1* enhancer, which represents a hallmark of the bipotent NMPs (Takemoto et al., 2011) (Figure S1A). We first measured changes in gene expression in EpiSCs after induction by Wnt3a or the Wnt agonist Chiron and Fgf, following a time course up to 72 hr. Typical markers for posterior axial extension, *Cdx2*, *T Bra*, *Wnt3a*, and *Cyp26a1*, were transcriptionally highly stimulated in comparison with their expression in non-treated EpiSCs (Figure 1B; Figure S1B), showing that EpiSCs exposed to Wnt and Fgf activate the pathways utilized by progenitors of axial tissues in vivo. Validation of EpiSCs as a reliable model for the elongating embryonic axis was further strengthened by the comparison of whole-transcriptome analysis of EpiSCs before and after Chiron and Fgf8 stimulation. RNA sequencing (RNA-seq) analysis uncovered 655 genes that were differentially expressed (false discovery rate [FDR] <0.05) (Table S1). Gene ontology (GO) analysis of significantly upregulated genes (fold change >2) revealed that the gene families that were affected were predominantly involved in pattern-specification processes and anteroposterior pattern formation (Figure 1C). *Cdx2* was one of the genes that was highly induced in the Chiron- and Fgf8-treated EpiSCs, and the protein showed homogeneous expression throughout the cell population (Figure 1D).

Direct Targets of Cdx2 in Wnt- and Fgf-Induced EpiSCs and Embryo Tail Buds

In order to identify the direct targets of Cdx2, ChIP-seq was performed using an anti-Cdx2 antibody in EpiSCs induced with Chiron and Fgf8 for 24 hr; 3,682 Cdx2-binding regions were identified from two replicates by MACS (Zhang et al., 2008) (Table S2). By performing motif analysis on regions 200 bp around the summit of peaks, the Cdx2 binding consensus sequence was found to be the top enriched motif (Figure 2A; Figure S2E). The majority of binding regions were localized distal to transcription start sites (Figure S2A). GO analysis of Cdx2 ChIP-seq binding regions (fold enrichment >5) using the GREAT "basal plus extension" rule (McLean et al., 2010) demonstrated enrichment of genes involved in processes associated with regionalization, AP patterning, and stem cell differentiation and development. Interestingly, the top signaling pathway-enriched term in the GO analysis was the Wnt signaling pathway (Figure 2B). Wnt pathway genes with active Cdx2-binding regions in their vicinity, as demonstrated by H3K27ac enrichment, are *Fzd10*, *Lef1*, and *Wnt5a* (Figure 2C). We assigned the 3,682 Cdx2-binding regions to a total of 3,970 genes using GREAT (Table S6).

To independently validate these Cdx2 targets in embryos in vivo, we also performed RNA-seq analysis in dissected tail buds of E8.0 Cdx mutant and wild type (WT) embryos. We compared the transcriptome of two- to five-somite-aged Cdx triple null embryos, which exhibit posterior truncation, with the transcriptome of *Cdx1-Cdx4* double mutants (*Cdx1-4* null), which are not impaired in their axial elongation, and that of age-matched WTs. We found that the sets of genes deregulated in Cdx null mutants versus WT, and in Cdx null mutants versus *Cdx1-4* null, were similar, whereas the comparison between *Cdx1-4* null and WT embryos uncovered only a few genes with a significant expression change (Figure 2E; Table S3); 172 genes were downregulated and 215 genes were upregulated in Cdx triple null compared to WT embryos (fold change >1.3; p value <0.05). This confirmed at the gene expression level that *Cdx2* is the key player in the process of axial elongation.

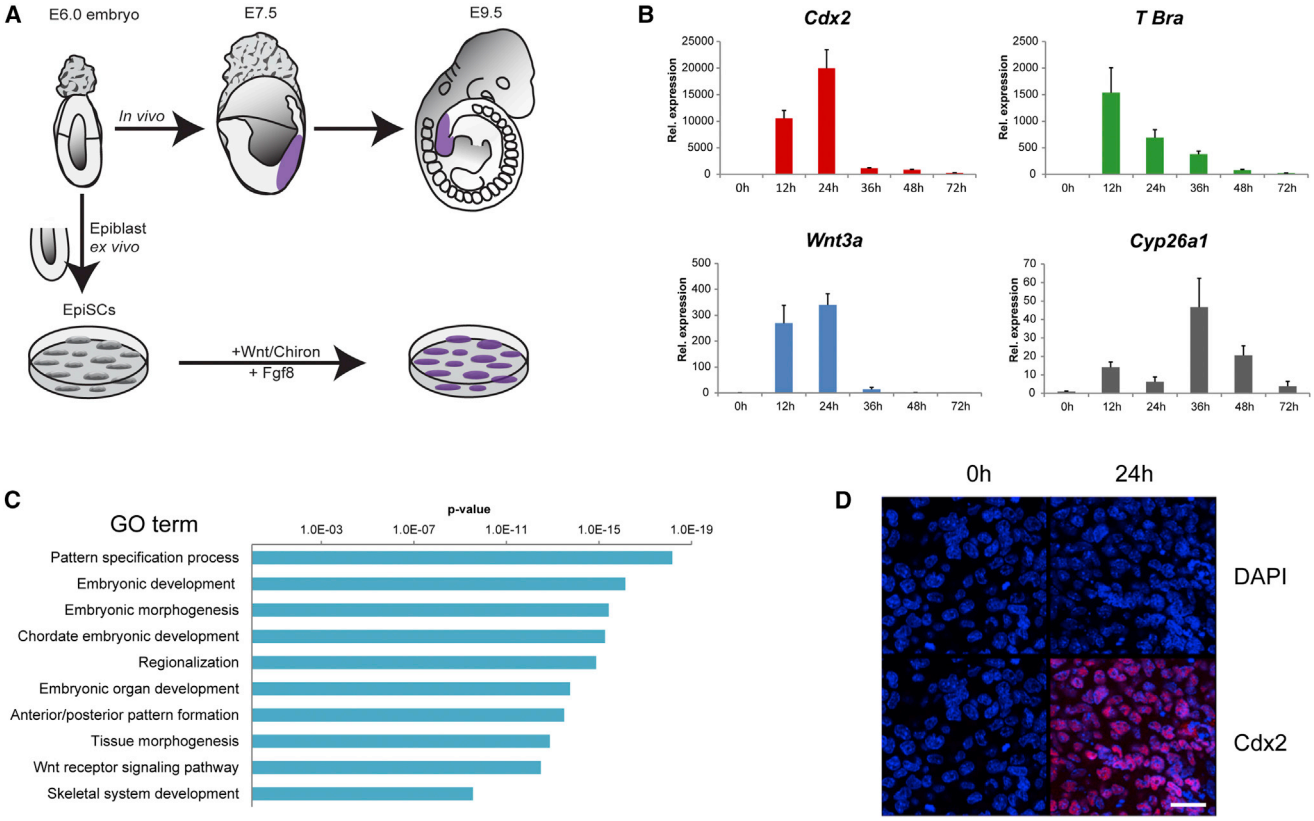

Figure 1. *Cdx2* Expression Is Induced by Wnt and Fgf Signaling in EpiSCs

(A) Induced EpiSCs as a model system for posterior embryonic development. Posterior gene expression is highlighted in purple.

(B) Induction time course of *Cdx2* expression and expression of markers for posterior axial extension upon Chiron stimulation for up to 72 hr. Values represent expression relative to 0 hr and normalized to the housekeeping gene *Ppia*. Error bars represent SD of at least two biological replicates.

(C) Top GO functional categories identified by DAVID analysis of RNA-seq upregulated genes in WT EpiSCs induced for 24 hr by Chiron/Fgf8. The length of the bars corresponds to the p value (x axis).

(D) Immunofluorescence staining using anti-Cdx2 antibody (red) in WT EpiSCs un-induced (0 hr) and induced (24 hr) with Chiron/Fgf8. Nuclear staining is blue (DAPI). Scale bar, 25 μm.

See also Figure S1.

Next, we determined the overlap between the set of Cdx2-bound loci revealed by the ChIP-seq experiments in WT EpiSCs and the up- and downregulated genes in the RNA-seq performed on Cdx triple mutant versus WT embryos (Figure 2D); 43.0% of the genes downregulated, and 27.4% of the genes upregulated in Cdx triple null mutant embryos, had at least one Cdx2-bound region assigned to them, suggesting that Cdx2 binding plays a more frequent direct role in gene activation. Most interestingly, several genes of the Wnt and Fgf pathways were bound by Cdx2 and downregulated in Cdx mutants (Figure 2E), convincingly demonstrating that Cdx2 directly stimulates these signaling pathways and that this stimulation is an essential and limiting step for embryonic posterior axial elongation.

A particular category of Cdx2 targets that is worth mentioning in the context of axial elongation concerns the Hox gene clusters. Cdx2 binds to the *Hox1–Hox9* subset of Hox genes in each cluster (Figures S2B and S2C), and these genes are upregulated in Wnt- and Fgf-induced EpiSCs and downregulated in Cdx triple null embryos with the exception of *Hoxa1* (Figure S2D). This is in line with the collaborative role of central Hox genes in axial elongation reported previously (Young et al., 2009). Given our previous genetic data on the antagonistic role of *Hox13* genes in the Cdx/Wnt/Fgf-supported axial elongation process at the trunk-to-tail transition in the mouse (van Rooijen et al., 2012; Young et al., 2009) and the inhibitory effect of Hox13 proteins on Wnt signaling documented in transient electroporation studies in chick embryos (Denans et al., 2015), we asked whether the direct targets of Cdx2 in the Wnt and Fgf pathways are also bound by Hox13 gene products. Binding-motif analysis for these Hox gene family transcription factors revealed that Hox13 proteins bind the same consensus sequence as Cdx proteins (Figure S2F). We previously demonstrated that precocious expression of Hox13 proteins, using the *Cdx2* promoter (*Cdx2P*), causes posterior truncation of the embryonic axis (Young et al., 2009). *Cdx2P-Hoxb13* homozygous mice manifested a moderate truncation of their tail. We used transgenic embryos from these mice to

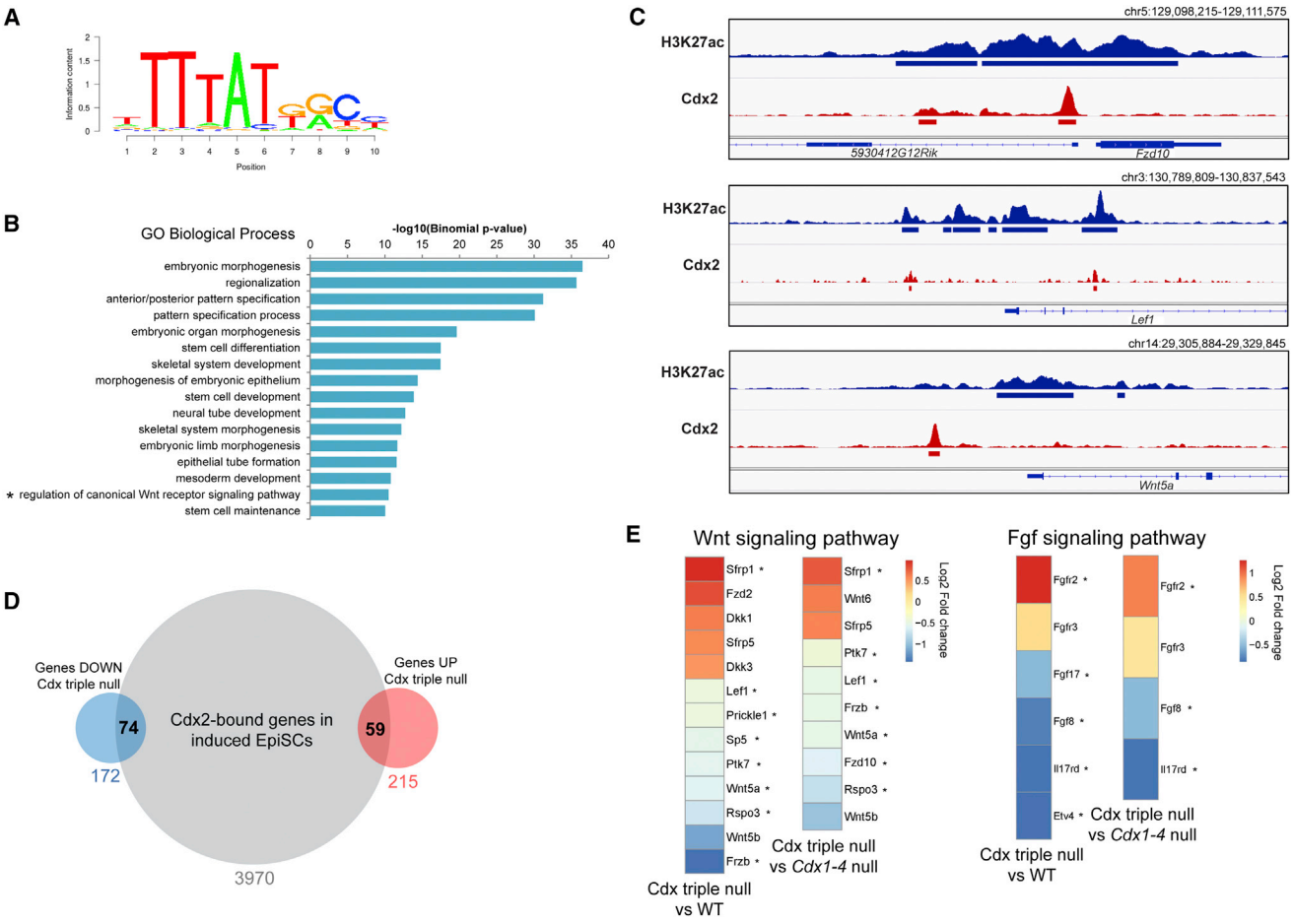

Figure 2. Cdx2 Directly Targets Genes in the Wnt and Fgf Signaling Pathways

(A) Sequence logo of the top enriched motif in Cdx2-bound 200-bp summit regions identified in induced EpiSCs by the SeqPos motif tool in Galaxy Cistrome.

(B) Top overrepresented "biological process" categories identified by GREAT analysis of top significant Cdx2 ChIP-seq binding regions. The length of the bars corresponds to the binomial raw (uncorrected) p value (x axis).

(C) ChIP-seq tracks for H3K27ac (blue) and Cdx2 (red) corresponding to the genomic regions containing *Fzd10*, *Lef1*, and *Wnt5a*. Solid bars under each track represent the MACS peak-calling identified regions.

(D) Overlap of genes identified by the basal plus extension association rule from Cdx2 ChIP-seq in induced WT EpiSCs (gray circle) with genes upregulated (red circle) and downregulated (blue circle) from Cdx triple null versus WT embryos in RNA-seq analyses.

(E) Differentially expressed genes in Cdx triple null versus WT and in Cdx triple null versus *Cdx1-4* null embryos linked to Wnt and Fgf signaling pathways with their corresponding $\log_2$ fold changes. Asterisks indicate genes bound by Cdx2 from ChIP-seq analysis in induced WT EpiSCs.

See also Figure S2.

investigate whether precocious Hoxb13 could exert its growth-antagonistic effect by binding to the Wnt and Fgf targets of Cdx2. We made use of the FLAG tag in front of the Hoxb13 N terminus (Figure S2G) to immunoprecipitate chromatin of dissected tail bud versus anterior trunk tissues of *Cdx2P-Hoxb13* embryos, and measured the enrichment of recovered DNA by qPCR for four different Cdx2 targets belonging to the Wnt and Fgf pathways (Figure S2H). This revealed that Hoxb13 binds these Cdx2 targets very efficiently in vivo. In addition, Cdx2 targets such as *T Bra*—a Cdx2 target essential for axial growth—is strongly downregulated by overexpression of *Hoxc13* in the posterior part of E10.5 transgenic embryos in vivo (Young et al., 2009). We conclude that the slowing down of axial elongation by Hox13 proteins may be executed by their direct binding to the same regulatory elements as Cdx2, and thereby arresting Cdx-dependent growth signaling.

Functional Validation of Cdx2 Direct Targets Involved in Embryonic Posterior Axial Elongation

To verify the involvement of a number of Cdx2-bound loci in the process of axial elongation in embryos, we determined whether the expression of these target genes was affected in Cdx triple null mutant embryos using in situ hybridization (ISH). Expression of *Fzd10*, *Wnt5a*, and *Fgf8* was decreased in the posterior parts of E8.0 mutant embryos compared to their age-matched controls (white arrows in Figure 3A and Figure S3A). Expression of Cdx2-bound genes was also quantified by qPCR in E7.5 WT

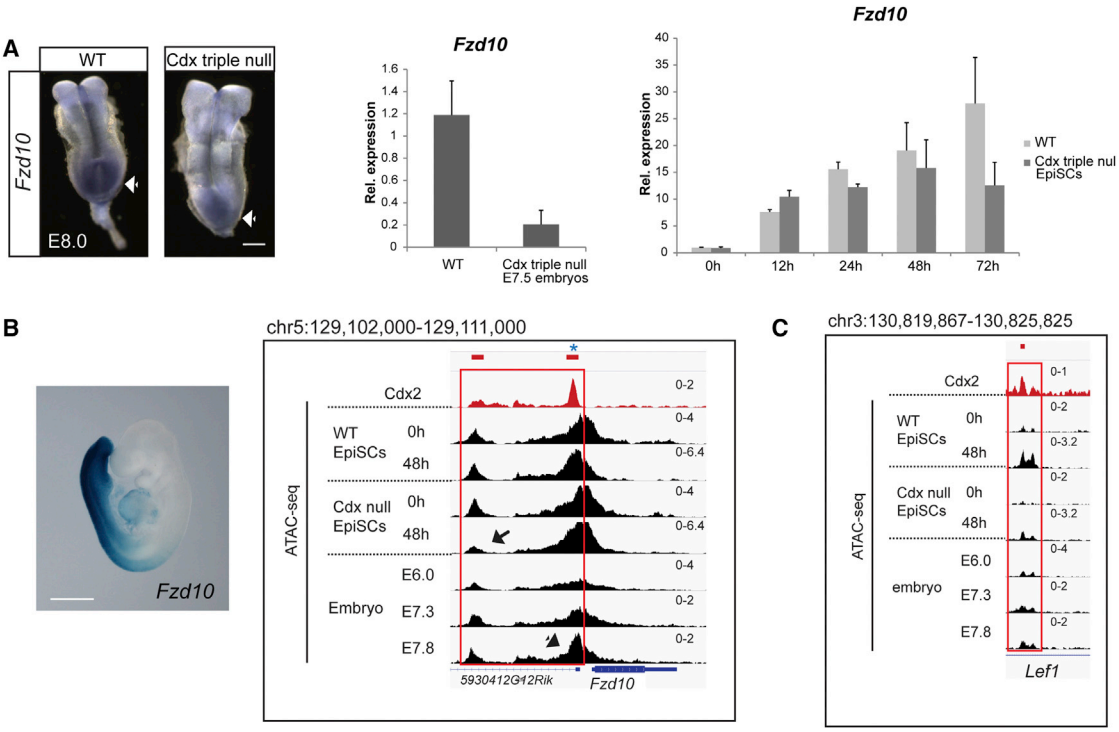

Figure 3. Cdx2 Directly Acts on Chromatin to Target Gene Transcription Involved in Embryonic Posterior Axial Elongation

(A) Left: ISH on E8.0 WT and Cdx triple null embryos using a *Fzd10* probe. White arrows indicate posterior expression. Scale bar, 100 μm. Right: *Fzd10* expression levels in WT and Cdx triple null E7.5 embryos. Values represent expression relative to the internal control gene. Induction time course of *Fzd10* expression in WT and Cdx triple null EpiSCs upon Chiron stimulation for up to 72 hr. Values represent expression relative to WT EpiSCs at 0 hr and normalized to *Ppia*. Error bars represent SD of at least two biological replicates.

(B) Left: activity of the Cdx2-bound *Fzd10* region coupled to a *lacZ* reporter in E9.5 embryos. Scale bar, 1 mm. Right: ATAC-seq profiles at the promoter region of *Fzd10* (red box) in un-induced and induced WT and Cdx triple null EpiSCs and in early embryos. The asterisk highlights the Cdx2-binding region tested in the *lacZ* reporter assay. The arrow shows less opening of the Cdx2-binding regions in induced Cdx triple null EpiSCs. The arrowhead shows this Cdx2-binding region is fully open in embryos when *Cdx2* expression is initiated. Red solid bars (above) represent the MACS peak-calling identified regions.

(C) ATAC-seq profiles at the *Lef1* locus.

See also Figure S3.

and Cdx triple null embryos, as well as in non-induced and induced WT and Cdx triple null EpiSCs, demonstrating that these genes are dependent on Cdx for their transcription (Figure 3A; Figure S3D).

Cdx2-binding regions were tested for enhancer activity using *lacZ* reporter assays in transgenic mice. The Cdx2-binding region upstream of *Fzd10* drives *lacZ* expression specifically in the posterior part of E9.5 transgenic embryos (Figure 3B). Furthermore, the Cdx2-binding regions identified near *Fgf8*, *Wnt5a*, and *Spry4-Fgf1* correspond to conserved genomic regions between human and mouse that have been validated previously as enhancers with posterior embryonic activity (Figure S3B; VISTA Enhancer Browser hs511, hs1472, and hs1640) (Visel et al., 2007).

DNA accessibility analysis (assay for transposase accessible chromatin with high-throughput sequencing [ATAC-seq]) showed that the Cdx2-binding regions near *Fgf8*, *Wnt5a*, *Spry4-Fgf1*, and *Rspo3* and, to a lesser extent, *Fzd10* are more accessible after induction of WT EpiSCs with Chiron and Fgf (Figure 3B; Figures S3B–S3D) (peaks distal to *Rspo3* were confirmed to be associated with the *Rspo3* promoter; data not shown). Similar results were found for a Cdx2 target site in the *Cdx2* regulatory region (Benahmed et al., 2008) and a region near *Lef1*, the gene encoding an executive transcription factor of the Wnt pathway (Figure 3C; Figure S3C). These Cdx2-bound regions become accessible in induced WT EpiSCs, whereas they do not become accessible in induced Cdx null EpiSCs. Moreover, most of these regions only become accessible in E7.8 embryos in vivo, consistent with the unavailability of Cdx proteins at earlier stages (Figures 3B and 3C; Figures S3B–S3D).

A more comprehensive analysis of Cdx2-dependent enhancers revealed that a large number of genes in the Wnt and Fgf pathways are bound by Cdx2 and also fail to become accessible in induced Cdx triple null EpiSCs (Table S4). Several of these genes also become accessible in E7.8 embryos (highlighted in Table S4). GO analysis revealed regions bound by Cdx2 that are inaccessible in Cdx triple null EpiSCs are enriched for genes associated with transcriptional regulation and include transcription factors that are essential for pattern specification (Table S4). These data suggest that Cdx2 could act as a pioneer transcription factor (Zaret and Mango, 2016) that initiates the expression of

important downstream target genes, among which are Wnt and Fgf signaling components.

Next, we determined the overlap between the set of regions that become accessible at E7.8 and those that fail to become accessible in induced Cdx null EpiSCs (Figure S3F). Seventy-nine percent (107 out of 136) of these enhancers do bind Cdx2, and become accessible in a Cdx-dependent way in EpiSCs and in embryos. This high percentage is also in line with a role of Cdx2 as a pioneer factor.

Opening of the chromatin at the Cdx2-binding enhancers, a prerequisite for target gene transcription in induced EpiSCs and in embryos, therefore depends in most cases on the presence of the Cdx protein. Collectively, these data indicate that Cdx2 binds to and activates enhancers of genes belonging to the Wnt and Fgf pathways, and that binding and activation are abolished in Cdx triple null EpiSCs and embryos.

Cdx2 and *T Bra* Are Co-expressed in the Posterior Axial Progenitor Region, and Double Mutants Exhibit a Truncated Phenotype More Severe Than Each Single Mutant

Inactivation of *Cdx2* and *T Bra* leads to a posterior truncation of the embryonic axis at a similar axial level. We therefore set out to compare the expression pattern of these two genes in detail. Expression of *Cdx2* in the embryo proper begins in the posterior part of the primitive streak at the late streak stage (E7.2). Expression then spreads rostrally along the streak in the epiblast and more weakly in the nascent mesoderm. Transcription of *Cdx2* is strong in the streak region and in the presomitic mesoderm at E8.5 and E9.5 (Figure S4A) and fades away by E12.5 (Young et al., 2009).

Initial expression of *T Bra* in the posterior part of the E6.0 egg cylinder precedes primitive streak appearance (Rivera-Pérez and Magnuson, 2005). *T Bra* is expressed in the epiblast abutting the streak and in the nascent mesoderm ingressing through the streak at E8.5 and E9.5 (Figure S4A). *T Bra* transcription is downregulated in the tail bud at the end of the axial extension around E14.5 (Cambray and Wilson, 2007). Both *Cdx2* and *T Bra* are expressed at high levels in posterior embryonic tissues during the developmental period between E7.5 and E10.5 that corresponds to the generation of trunk tissues (Figure 4A). Both genes start to be downregulated around the trunk-to-tail transition, resulting in a drop of transcription around E12.5 for *Cdx2* and E14.5 for *T Bra*.

Examination of the distribution of the active chromatin mark H3K27ac in the neighborhood of *Cdx2* and *T Bra* confirms that these loci are active in E9.5 embryonic tail bud tissues, whereas they are not in anterior tissues of the same embryos (Figure 4B). Moreover, a similar H3K27ac profile is observed in induced EpiSCs (Figure 4B), confirming that these EpiSCs are a valid model for the posteriorly elongating embryonic tissues.

Cdx2 null mutant embryos are arrested after 7–12 somites (van de Ven et al., 2011). *T Bra* null embryos do not generate more than about 7 somites, and their neural tube at posterior levels is kinked and abnormal (Rashbass et al., 1994) (Figure S4B). Double-mutant embryos were generated from intercrosses of *Cdx2* conditional homozygotes carrying a null allele of *T Bra* and a *Rosa26-Cre ER(T2)* allele. These embryos clearly exhibit a more severely truncated phenotype posteriorly than each single mutant (Figure 4C). Furthermore, double mutants are missing all posterior tissues that form a tail bud in the WT and single mutants (highlighted in Figure 4C). In the mesoderm that is generated, only three to five disorganized somites can be discerned after ISH with the somitic marker *Mox1* (Figure 4C, lower panels). The *T Bra* null mutation affects somite morphogenesis, as visible in *T Bra* null and *Cdx2* null/*T Bra* null embryos. Embryos lacking both functional *Cdx2* and *T Bra* generate head and occipital structures exclusively. *Cdx2* and *T Bra* thus cooperate in their action in such a way that missing both genes together is much more deleterious for growth of the embryonic trunk than missing each one at a time.

In order to further understand the basis of the *Cdx2*/*T Bra* double-mutant phenotype, we examined the distribution of the Cdx2 and T Bra proteins in the posterior part of the embryo from which the axis extends. Co-staining of transverse sections of the posterior part of E8.5 embryos with antibodies against T Bra and Cdx2 demonstrates that both proteins are present at the same location where NMPs are known to reside (Figure 4D). Cdx mutants, like *T Bra* mutants, form ectopic neural structures at posterior levels (van de Ven et al., 2011; Yamaguchi et al., 1999) (Figure S4D), strengthening the notion that both of these genes control the NMP-dependent growth of the posterior embryonic axis. Mutants in the niche factor Wnt3a also exhibit posterior ectopic neural structures (Yoshikawa et al., 1997), indicating that these transcription factors and signaling pathways act in the same network to orchestrate axial extension by modulating the NMP population.

Cdx2 and T Bra Collaborate in Directly Activating a Wnt and Fgf Gene Regulatory Network

Previous work has shown that mouse Cdx (Bialecka et al., 2010; van de Ven et al., 2011) and zebrafish *T Bra* (Martin and Kimelman, 2008, 2010) affect axial elongation at least in part by impairing the posterior progenitor niche. We find that *T Bra* and *Cdx2* in the mouse are co-expressed in the NMP region from which axial tissue expands throughout the duration of trunk axial elongation. Our observations that *Cdx2* null and *T Bra* null mutations add their effects in impairing axial elongation of the embryonic trunk prompted us to test whether Cdx2 and T Bra stimulate posterior growth signaling by co-activating genes of the Wnt and Fgf pathway.

Cdx2 and *T Bra* are strongly transcribed in the posterior tissues of E7.5 until E10.5 embryos (Figure 4A; Figure S4A). Several genes of the Wnt and Fgf pathways, among which are *Wnt3a* and *Fgf8*, are also expressed in posterior embryonic tissues, similar to Cdx2 and *T Bra* (Figure S5A). We therefore performed ChIP-seq for T Bra in induced EpiSCs to investigate whether there are common targets for T Bra and Cdx2 in embryonic posterior tissues. We identified 1,215 T Bra-binding regions from two replicates by MACS (Zhang et al., 2008) (Table S5). The T Bra-binding motif (Kispert and Herrmann, 1993) is one of the top enriched motifs in the uncovered binding regions, 200 bp around the summit of the peaks (Figure 5A). The other motifs correspond to the binding sequences of other T box transcription factor-encoding genes (Figure S5C). GO analysis of T Bra ChIP-seq data showed

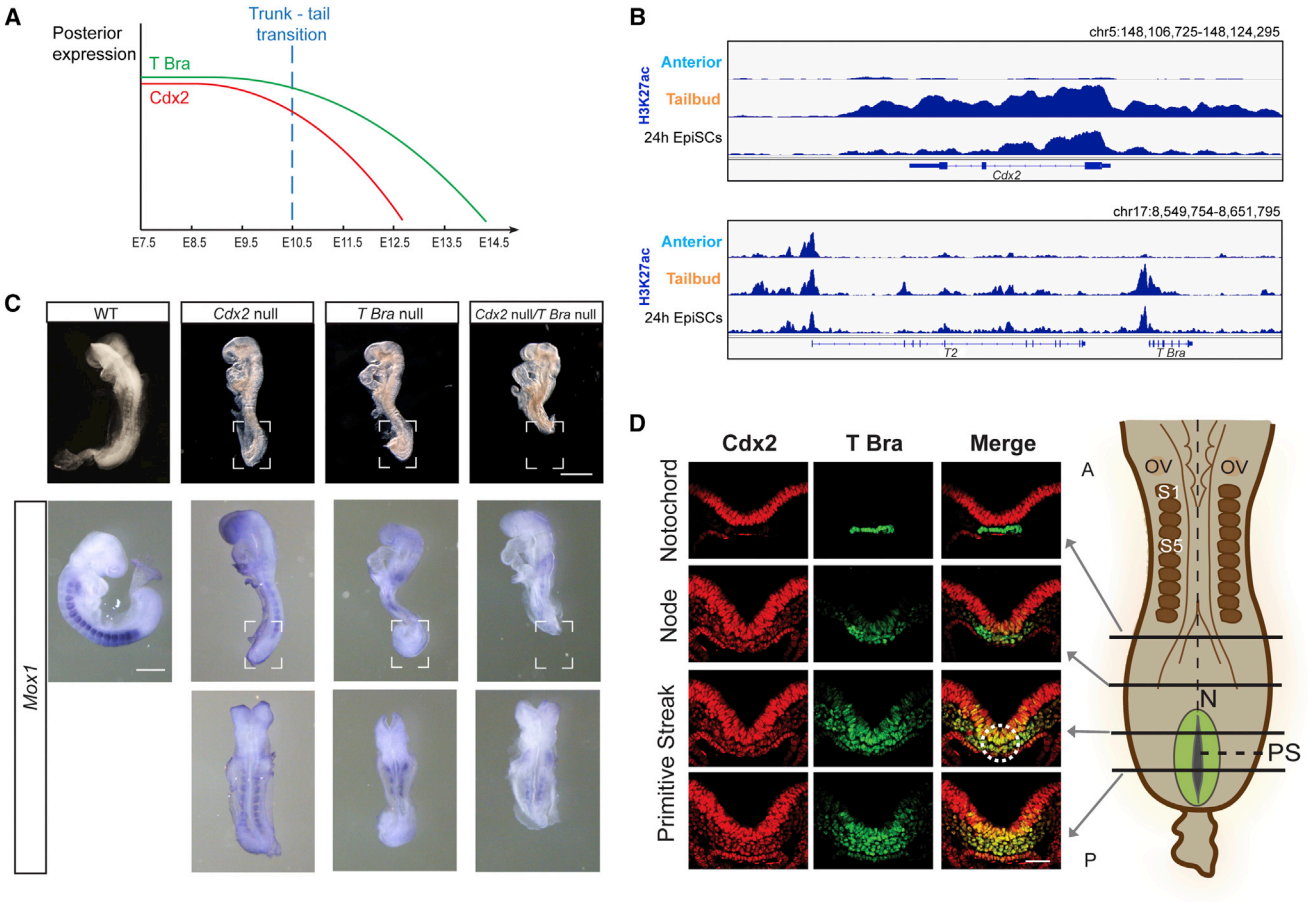

Figure 4. *Cdx2* and *T Bra* Are Co-expressed in the Axial Progenitor Region and Collaborate in Driving Axial Extension

(A) Schematic representation of the expression level of *Cdx2* (red) and *T Bra* (green) in the posterior part of developing embryos. Developmental stages are along the x axis; the trunk-to-tail transition is indicated (blue dashed line).

(B) H3K27ac ChIP-seq tracks corresponding to the genomic regions containing *Cdx2* (top panels) and *T2*/*T Bra* (bottom panels) in anterior tissue, tail bud tissue, and WT EpiSCs induced for 24 hr with Chiron/Fgf8.

(C) Top panel (left to right): WT, *Cdx2* null, *T Bra* null, and *Cdx2* null/*T Bra* null E8.5 embryos. The WT embryo has 12 somites, the *Cdx2* null embryo shown here has 10 somites, the *T Bra* null embryo has 6 recognizable somites, and the *Cdx2* null/*T Bra* null mutant embryo has 4 or 5 identifiable somites. Scale bar, 200 μm. Bottom: expression of the somite marker *Mox1* in WT and mutant embryos by ISH. The WT embryo has 15 somites, the *Cdx2* null embryo shown here has 7 or 8 somites, the *T Bra* null embryo has 5 recognizable somites, and the *Cdx2* null/*T Bra* null mutant embryo has 4 identifiable somites. White brackets highlight tissue missing in *Cdx2* null/*T Bra* null mutant embryos. Scale bar, 100 μm.

(D) Left: Cdx2 and T Bra immunofluorescence staining on transversal sections of the posterior region of the wild-type mouse embryo at E8.0. The axial progenitors (NMPs) reside at the level between the anterior primitive streak and the node-streak border (NSB, white dotted circle). Scale bar, 50 μm. Right: graphic of the posterior part of the embryo; black solid lines represent the level of each section, and the posterior growth zone is highlighted in green. A, anterior; P, posterior; N, node; OV, otic vesicle; S, somite PS, primitive streak.

See also Figure S4.

enrichment for genes expressed in the mesoderm and primitive streak (Figure 5B) with peaks distal to transcription start sites (Figure S5B). When comparing the series of T Bra- and Cdx2-bound regions, a number of common target genes were identified (Figure 5C). Importantly, among these common targets are several genes belonging to the Wnt and Fgf pathways, including Wnt ligands (Figure S5D; Table S6). These were all associated by at least some criteria with activation of their target gene expression in embryos and in EpiSCs (Figure S5D). Upon examination of the list of these common targets of Cdx2 and T Bra together versus Cdx2 and T Bra alone (Table S6), it appears that Cdx2 binds many more loci in the Wnt and Fgf pathways than T Bra does. Notably, T Bra and Cdx2 bind to each other's gene locus (Table S6) without affecting each other's transcription in single-mutant embryos (Chawengsaksophak et al., 2004; Lolas et al., 2014; van de Ven et al., 2011). Nevertheless, according to our RNA-seq data and previous work, *T Bra* is significantly downregulated in Cdx triple-mutant embryos (Table S3) (van Rooijen et al., 2012).

Some loci binding both Cdx2 and T Bra exhibit binding of these factors at non-overlapping sites, for example *Myc*, *Tle3*, and *Tcf7l2* (Figure 5D). For these genes, ATAC-seq experiments

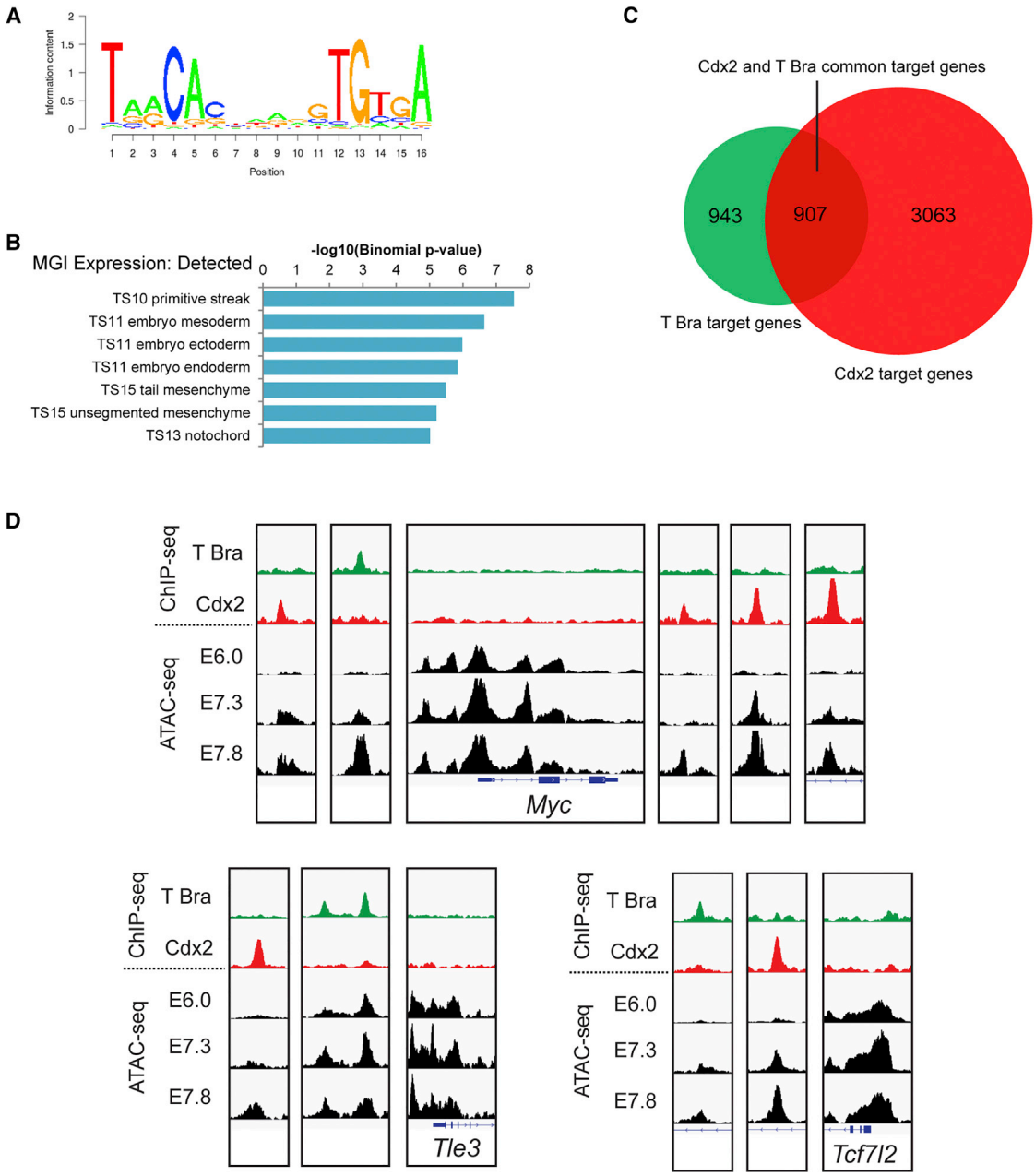

Figure 5. Cdx2 and T Bra Bind Common Genes of the Wnt and Fgf Signaling Pathways

(A) Sequence logo of the top enriched motif in T Bra-bound 200-bp summit regions identified in induced EpiSCs by the SeqPos motif tool in Galaxy Cistrome.

(B) Top overrepresented "MGI expression: detected" categories identified by GREAT analysis of T Bra ChIP-seq binding regions. The length of the bars corresponds to the binomial raw (uncorrected) p value (x axis). TS, Theiler stage.

(C) Overlap of Cdx2- and T Bra-bound genes identified by the GREAT basal plus extension gene association rule.

(D) ATAC-seq profiles at *Myc*, *Tle3*, and *Tcf7l2* loci in embryos at increasing developmental stages.

See also Figure S5.

demonstrated that chromatin accessibility increases at both Cdx2 and T Bra peaks in embryos at stages when NMPs contribute to trunk axial extension compared to early embryos (Figure 5D). A subset of the genes that bind both Cdx2 and T Bra do so in regions that also exhibit enhancer properties (H3K27ac enrichment and/or open chromatin) (Figure 6A).

Loci that bind T Bra only were *Foxa2* (found to bind T Bra in humans as well) (Faial et al., 2015) and *Mesp1*, *Mesp2*, *Ripply2*, and *Tbx6*. The latter targets concern an independent additional function for T Bra in regulating mesoderm fate, which Cdx2 does not share (Figure S5E). This explains the difference in appearance of the posterior tissues when *T Bra* is inactive.

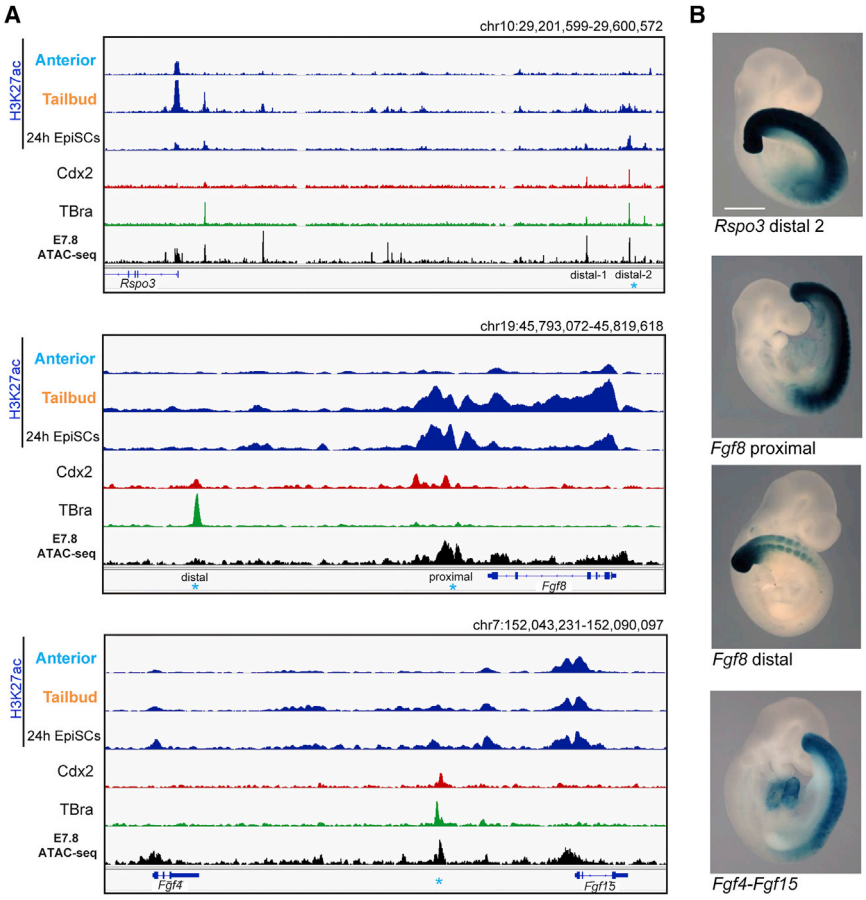

Figure 6. Cdx2- and T Bra-Co-bound Regions Activate Genes of the Wnt and Fgf Signaling Pathways In Vivo

(A) ChIP-seq for H2K27ac, Cdx2, and T Bra and ATAC-seq for E7.8 embryos in the genomic regions containing *Rspo3* (top panels), *Fgf8* (middle panels), and *Fgf4-Fgf15* (bottom panels). Embryo tracks are in bold. Asterisks indicate regions further tested in *lacZ* transgenic assays.

(B) Activity of Cdx2- and T Bra-co-bound regions coupled to the *lacZ* reporter in E9.5 WT embryos. Top: *Rspo3* distal enhancer 2; middle: *Fgf8* proximal enhancer and *Fgf8* distal enhancer; bottom: *Fgf4-Fgf15* enhancer. Scale bar, 1 mm.

(C) Cdx2 and T Bra occupancy by ChIP-qPCR in posterior versus anterior E9.5 embryonic tissues. Enrichment of each region following immunoprecipitation with anti-Cdx2 and anti-T Bra antibody is calculated as fold enrichment over negative anterior embryonic tissue. Neg chr3 is a negative control region.

See also Figure S6.

To functionally validate the involvement of commonly bound regions in genes of the Wnt and Fgf pathways by T Bra and Cdx2 in vivo, we performed *lacZ* reporter assays to test their activity. These assays confirmed that the T Bra- and Cdx2-co-bound regions near *Rspo3*, *Fgf8*, and *Fgf4-Fgf15* specifically activate gene transcription in the posterior region of E9.5 embryos (Figure 6B). Interestingly, Cdx2 binding sites identified by our Cdx2 ChIP-seq were more conserved than T Bra binding sites, and common binding sites were highly conserved (Figure S6A). The sequences corresponding to the peaks that were tested in *lacZ* assays were also found to be strongly conserved evolutionarily between human and mouse (Figure S6B). Validation of Cdx2 and T Bra enrichment at these latter loci was performed by ChIP-qPCR in embryonic tail bud versus anterior tissues at E9.5 (Figure 6C). Binding of both Cdx2 and T Bra to regions corresponding to the genes of the Wnt and Fgf pathways discovered in our ChIP-seq experiments was found to be exclusive for posterior embryonic tissues (Figure 6C). The data collectively demonstrate that Cdx2 and T Bra bind together to genes of the Wnt and Fgf pathway and that this binding causes target gene activation, a prerequisite for maintenance of the posterior progenitor niche in embryos.

DISCUSSION

Cdx, T Bra, and Axial Extension from Posterior Progenitors

In the mouse embryo, trunk tissues are formed from populations of progenitors arising within the epiblast at the beginning of somitogenesis. Progenitors located between the node and the anterior end of the primitive streak, called the node-streak border (NSB), have been shown to constitute a population of stem cell-like NMPs (Cambray and Wilson, 2002, 2007) that contribute descendants to long axial distances. These NMPs were defined by co-expressing *T Bra* and *Sox2*. Epiblast cells abutting the NMP region posteriorly on both sides of the primitive streak have been called the caudo-lateral epiblast (CLE) (Wilson et al., 2009). The progenitors in the most posterior part of the CLE and NMP regions differ in their dependence on signaling pathways. Canonical Wnt was shown to regulate the size of the NMP population (Wymeersch et al., 2016) and is believed to maintain this progenitor pool, whereas the mesoderm progenitors in the posterior CLE are less dependent on this signaling. These data set the stage on which the action of T Bra and Cdx2 play their role in ensuring trunk and posterior axial extension from the posterior progenitor populations by sustaining Wnt and Fgf signaling in the

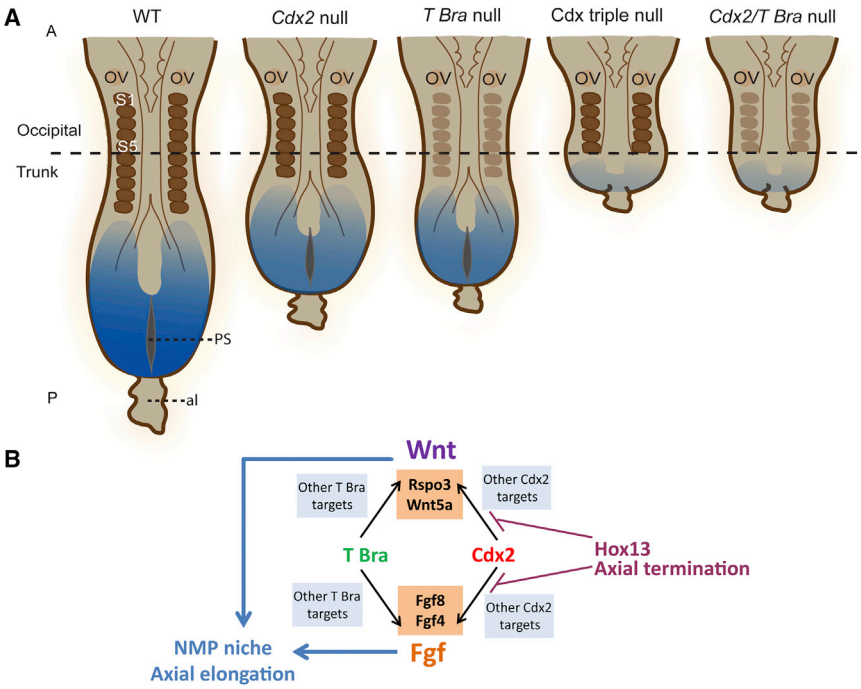

Figure 7. Schematic Representation of the Loss of Wnt and Fgf Signaling in Cdx and *T Bra* Mutant Embryos and the Model for Maintenance of the Niche

(A) Schematic dorsal view of E8.5 (left to right) WT, *Cdx2* null, *T Bra* null, Cdx triple null, and *Cdx2* null/*T Bra* null mutant embryos. The Wnt and Fgf signaling gradient is in blue. Somites are formed irregularly in *T Bra* mutants (light brown). Al, allantois.

(B) Model of the *Cdx2*, *T Bra*, Wnt, and Fgf gene regulatory network to maintain the niche for axial extension. Hox13 binds to Cdx2 targets to antagonize Cdx2 action and contributes to axial termination.

NMP niche. The co-expression of Cdx and T Bra in NMPs and their niche, the *Cdx2* and *T Bra* mutant phenotypes, their rescue by Wnt, and the binding of Cdx and T Bra at Wnt pathway loci all suggest that these transcription factors regulate the NMPs and anterior CLE populations of progenitors. Besides NMP pool amplification and maintenance, Wnt signaling plays an additional role in driving the differentiation choice of NMPs. The *T Bra* and *Cdx2* loss of function and precocious expression of Hox13 affect this differentiation choice of the NMPs as shown by the fact that in all these situations, ectopic neural tissues are formed posteriorly in embryos. The data collectively establish *Cdx2* expression as an essential factor in the signature of NMPs, together with T Bra. Interestingly, T Bra/Ntl was reported to bind to genes specifying posterior fate in zebrafish embryos (Morley et al., 2009), one of which was *cdx4*. T Bra and Cdx therefore may belong to an evolutionarily conserved mechanism driving NMP development. In addition, our data indicate that Cdx2 is likely to act as a pioneer transcription factor on genes that maintain the niche of these NMPs.

Both Cdx2 and T Bra Directly Activate Genes Sustaining Posterior Axial Elongation in NMPs and Their Niche

Cdx2 and T Bra proteins are essential for NMP maintenance in the embryonic posterior growth zone. The NMP niche is dependent on both Wnt and Fgf, as proven from the posterior truncation phenotype of mutants in the Wnt (Galceran et al., 1999; Takada et al., 1994) and Fgf pathways (Hoch and Soriano, 2006; Naiche et al., 2011). The functional activation of Wnt and Fgf pathway loci upon binding of Cdx2 and T Bra indicates that these transcription factors are actively contributing to axial growth at the time embryos generate their trunk. Our ChIP-seq experiments identify some of the ligands and agonists of the Wnt and Fgf pathways that are directly targeted by both Cdx2 and T Bra. As reported for adult intestinal stem cells (Clevers et al., 2014), we conclude that *Cdx2*- and *T Bra*-expressing NMPs stimulate and maintain their own niche.

Collaboration of Cdx and T Bra in Embryonic Trunk Morphogenesis

The Cdx genes are required for the generation of the complete post-occipital part of the axis. This is in line with Cdx genes being paraHox genes (sharing ancestry with the Hox genes), exclusively involved in the generation and patterning of the trunk and posterior tissues. Despite the fact that *T Bra* is expressed much earlier than when NMPs start contributing to trunk elongation (early somite stage; Wymeersch et al., 2016), T Bra null mutants generate a normal anterior part of their axis, including occipital tissues and the first seven somites. It has been proposed that other T box genes that bind the same motif as T Bra possibly account for the axial growth during the generation of the anterior set of somites in *T Bra* null mutants (Gentsch et al., 2013). Whatever it may be, *Cdx2* loss of function reduces the amount of posterior axial tissue made in *T Bra* mutants to the remaining occipital section of the axis in the compound mutants. The fact that the double mutants lacking both Cdx2 and T Bra exhibit a severe posterior truncation at the same axial level as the Cdx null mutants (Figure S4C) suggests that the action of Cdx2 on posterior tissue generation is similarly supplemented by either Cdx1 and Cdx4, as shown before (van Rooijen et al., 2012), or by T Bra. This results from the fact that two partially redundant systems, T Bra and Cdx, converge in their output on the growth signaling activity in the axial progenitor niche. This is illustrated in Figure 7A.

Cdx, T Bra, and the Hox Genes Instruct the Trunk-to-Tail Transition and the Termination of Axial Growth

T Bra and Cdx2 are indispensable driving forces for trunk axis extension. Previous work showed that genes in the middle region of the Hox clusters could assist Cdx in supporting trunk axial growth (Young et al., 2009). We found that Cdx2 binds to many sites in the anterior and middle part of the Hox clusters in EpiSCs and in embryos, and upregulates these genes in both these systems. This upregulation, added to the autoregulation of Cdx2 and to its cross-regulation by T Bra, insures a robust output of

Cdx and Hox stimulators on trunk axial growth. The situation changes after the trunk-to-tail transition. Cdx genes are downregulated by E12.5 and *T Bra* by E14.5. In addition, the posterior Hox genes, such as Hox13, which are turned on later than the anterior and central genes of the clusters, are expressed at high levels in the growth zone after the trunk-to-tail transition. Hox13 gene products have been shown to repress axial growth when expressed precociously, antagonizing the action of anterior and central Hox and Cdx genes (Young et al., 2009). A repressive function of Hox13 on more anterior Hox genes was recently demonstrated mechanistically for HoxA genes in the limb (Beccari et al., 2016). Due to this repressive function, Hox13 proteins would interrupt the transcription of any anterior and central Hox gene that would still be expressed in the growth zone after the trunk-to-tail transition. This negative regulation of Hox13 on more anterior Hox genes would occur spatially in the region where NMPs are located. In addition, our data show binding of Hox13 and Cdx2 on the same genes of the growth signaling pathways. We therefore propose that the Cdx2/Hox trunk-stimulating loop is weakened at the trunk-to-tail transition by the dual action of Hox13 proteins that on one end repress more anterior Hox genes and on the other end antagonize Cdx2 binding. In addition to the downregulation of T Bra and Cdx (Young et al., 2009), this reduces Wnt and Fgf signaling in the growth zone, exhausting the niche of the NMPs, and foreshadowing the termination of axial elongation (Figure 7A).

This study establishes Cdx2 as a key transcriptional component that collaborates with T Bra in the maintenance of the NMPs and their niche during trunk axial elongation in embryos (Figure 7B). In addition to being downregulated after the trunk-to-tail transition, Cdx2 is counteracted by Hox13 proteins, ensuring axis extension termination.

EXPERIMENTAL PROCEDURES

Mouse Strains

All experiments using mice were performed in accordance with institutional and national guidelines and regulations, under the control of the Dutch Committee for Animals in Experiments. All mice were in the C57Bl6j/CBA mixed background. The *Cdx2* conditional allele was described previously (Stringer et al., 2012) and the *T Brachyury*^{2J} deletion allele was described previously (Herrmann et al., 1990). Details of all transgenic mice are described in Supplemental Experimental Procedures. ISH of transcripts in mouse embryos was performed as described previously (Young et al., 2009).

EpiSC Derivation and Culture

WT and Cdx triple null pre-streak embryos (E6.0) were isolated in M2 medium; extraembryonic tissue and surrounding primitive endoderm were removed as described previously (Neijts et al., 2016). Detailed cell-culture and induction procedures are described in Supplemental Experimental Procedures.

RNA-Seq

Mouse embryos were isolated at E8.0 as described previously (Young et al., 2009); eight dissected tail buds were pooled for each replicate (three- to five-somite stage). For mRNA sequencing, 10 ng of total RNA was used as starting material and processed using the CEL-Seq protocol (Hashimshony et al., 2012) described in Supplemental Experimental Procedures.

ChIP and ChIP-Seq

ChIP-seq was performed on EpiSCs according to a standard ChIP protocol. Detailed ChIP-seq analysis is described in Supplemental Experimental Procedures. ChIP on 50 E9.5 tail bud and anterior mouse embryonic tissue was performed as described previously (Amin and Bobola, 2014). For differential posterior versus anterior E9.5 embryonic tissues, posterior tissues were the posterior parts of the embryos dissected at the level of the last formed somite, and anterior tissues were taken between the branchial arches and forelimb bud. Antibodies are described in Supplemental Experimental Procedures.

ATAC-Seq

ATAC-seq was performed as described previously (Neijts et al., 2016).

Statistical Analysis

For ChIP-seq experiments, statistically significant enriched regions for Cdx2, T Bra, and H3K27ac were identified using MACS (Zhang et al., 2008) with a p value threshold of 10^{-5}. For RNA-seq experiments, statistically significant differentially expressed genes were identified using DESeq2 (Love et al., 2014). An FDR of <0.05 was used. For heterogeneous embryonic material, genes with a p value of <0.05 were identified.

ACCESSION NUMBERS

The accession numbers for the ChIP-seq, RNA-seq, and ATAC-seq data reported in this paper are GEO: GSE84899 and GSE81203.

SUPPLEMENTAL INFORMATION

Supplemental Information includes Supplemental Experimental Procedures, six figures, and six tables and can be found with this article online at http://dx.doi.org/10.1016/j.celrep.2016.11.069.

AUTHOR CONTRIBUTIONS

J.D., S.A., R.N., and S.S. conceived the study. S.A., R.N., S.S., and C.v.R. performed the experiments. S.A. performed the ChIP experiments, RNA-seq experiments, and next generation sequencing (NGS) data analysis. R.N. generated and characterized EpiSCs and performed the ATAC-seq experiments. S.S. generated the *Cdx2/T Bra* double-mutant embryos. C.v.R. generated the Cdx triple null mice and performed the ISH experiments. S.C.T. performed the bioinformatics analyses of ChIP-seq, RNA-seq, and ATAC-seq data. L.K. processed the samples for RNA-seq, according to the technology developed in the A.v.O. laboratory. M.P.C. provided expert advice on some of the ChIP-seq experiments. S.A. and J.D. wrote the manuscript.

ACKNOWLEDGMENTS

We thank Jeroen Korving for micro-injection of the *lacZ* reporter constructs. We thank Deneen Wellik for providing us with the *Hoxb13 FLAG* expression construct, and Joris Slingerland for characterizing the homozygous animals of our *Cdx2P-Hoxb13 FLAG* mouse colonies. We thank Guilherme Costa and Wim de Graaff for some of the ISHs, and Fabrizio Giuliani for help with immunostaining in one of the experiments. We thank Marit W. Vermunt for help with bioinformatics analysis. This work was supported by a grant from the Netherlands Institute for Regenerative Medicine (NIRM, grant FES0908).

Received: August 11, 2016
Revised: October 26, 2016
Accepted: November 18, 2016
Published: December 20, 2016

REFERENCES

Amin, S., and Bobola, N. (2014). Chromatin immunoprecipitation and chromatin immunoprecipitation with massively parallel sequencing on mouse embryonic tissue. Methods Mol. Biol. *1196*, 231–239.

Beccari, L., Yakushiji-Kaminatsui, N., Woltering, J.M., Necsulea, A., Lonfat, N., Rodríguez-Carballo, E., Mascrez, B., Yamamoto, S., Kuroiwa, A., and Duboule,

D. (2016). A role for HOX13 proteins in the regulatory switch between TADs at the HoxD locus. Genes Dev. *30*, 1172–1186.

Benahmed, F., Gross, I., Gaunt, S.J., Beck, F., Jehan, F., Domon-Dell, C., Martin, E., Kedinger, M., Freund, J.N., and Duluc, I. (2008). Multiple regulatory regions control the complex expression pattern of the mouse Cdx2 homeobox gene. Gastroenterology *135*, 1238–1247.e3.

Bialecka, M., Wilson, V., and Deschamps, J. (2010). Cdx mutant axial progenitor cells are rescued by grafting to a wild type environment. Dev. Biol. *347*, 228–234.

Cambray, N., and Wilson, V. (2002). Axial progenitors with extensive potency are localised to the mouse chordoneural hinge. Development *129*, 4855–4866.

Cambray, N., and Wilson, V. (2007). Two distinct sources for a population of maturing axial progenitors. Development *134*, 2829–2840.

Chawengsaksophak, K., James, R., Hammond, V.E., Köntgen, F., and Beck, F. (1997). Homeosis and intestinal tumours in Cdx2 mutant mice. Nature *386*, 84–87.

Chawengsaksophak, K., de Graaff, W., Rossant, J., Deschamps, J., and Beck, F. (2004). Cdx2 is essential for axial elongation in mouse development. Proc. Natl. Acad. Sci. USA *101*, 7641–7645.

Clevers, H., Loh, K.M., and Nusse, R. (2014). Stem cell signaling. An integral program for tissue renewal and regeneration: Wnt signaling and stem cell control. Science *346*, 1248012.

Denans, N., Iimura, T., and Pourquié, O. (2015). Hox genes control vertebrate body elongation by collinear Wnt repression. eLife *4*, e04379.

Faial, T., Bernardo, A.S., Mendjan, S., Diamanti, E., Ortmann, D., Gentsch, G.E., Mascetti, V.L., Trotter, M.W., Smith, J.C., and Pedersen, R.A. (2015). Brachyury and SMAD signalling collaboratively orchestrate distinct mesoderm and endoderm gene regulatory networks in differentiating human embryonic stem cells. Development *142*, 2121–2135.

Galceran, J., Fariñas, I., Depew, M.J., Clevers, H., and Grosschedl, R. (1999). Wnt3a(−/−)-like phenotype and limb deficiency in Lef1(−/−)Tcf1(−/−) mice. Genes Dev. *13*, 709–717.

Gentsch, G.E., Owens, N.D., Martin, S.R., Piccinelli, P., Faial, T., Trotter, M.W., Gilchrist, M.J., and Smith, J.C. (2013). In vivo T-box transcription factor profiling reveals joint regulation of embryonic neuromesodermal bipotency. Cell Rep. *4*, 1185–1196.

Gouti, M., Tsakiridis, A., Wymeersch, F.J., Huang, Y., Kleinjung, J., Wilson, V., and Briscoe, J. (2014). In vitro generation of neuromesodermal progenitors reveals distinct roles for Wnt signalling in the specification of spinal cord and paraxial mesoderm identity. PLoS Biol. *12*, e1001937.

Hashimshony, T., Wagner, F., Sher, N., and Yanai, I. (2012). CEL-Seq: single-cell RNA-seq by multiplexed linear amplification. Cell Rep. *2*, 666–673.

Herrmann, B.G., Labeit, S., Poustka, A., King, T.R., and Lehrach, H. (1990). Cloning of the T gene required in mesoderm formation in the mouse. Nature *343*, 617–622.

Hoch, R.V., and Soriano, P. (2006). Context-specific requirements for Fgfr1 signaling through Frs2 and Frs3 during mouse development. Development *133*, 663–673.

Kispert, A., and Herrmann, B.G. (1993). The Brachyury gene encodes a novel DNA binding protein. EMBO J. *12*, 3211–3220.

Lolas, M., Valenzuela, P.D., Tjian, R., and Liu, Z. (2014). Charting Brachyury-mediated developmental pathways during early mouse embryogenesis. Proc. Natl. Acad. Sci. USA *111*, 4478–4483.

Love, M.I., Huber, W., and Anders, S. (2014). Moderated estimation of fold change and dispersion for RNA-seq data with DESeq2. Genome Biol. *15*, 550.

Martin, B.L. (2016). Factors that coordinate mesoderm specification from neuromesodermal progenitors with segmentation during vertebrate axial extension. Semin. Cell Dev. Biol. *49*, 59–67.

Martin, B.L., and Kimelman, D. (2008). Regulation of canonical Wnt signaling by Brachyury is essential for posterior mesoderm formation. Dev. Cell *15*, 121–133.

Martin, B.L., and Kimelman, D. (2009). Wnt signaling and the evolution of embryonic posterior development. Curr. Biol. *19*, R215–R219.

Martin, B.L., and Kimelman, D. (2010). Brachyury establishes the embryonic mesodermal progenitor niche. Genes Dev. *24*, 2778–2783.

McLean, C.Y., Bristor, D., Hiller, M., Clarke, S.L., Schaar, B.T., Lowe, C.B., Wenger, A.M., and Bejerano, G. (2010). GREAT improves functional interpretation of *cis*-regulatory regions. Nat. Biotechnol. *28*, 495–501.

Morley, R.H., Lachani, K., Keefe, D., Gilchrist, M.J., Flicek, P., Smith, J.C., and Wardle, F.C. (2009). A gene regulatory network directed by zebrafish No tail accounts for its roles in mesoderm formation. Proc. Natl. Acad. Sci. USA *106*, 3829–3834.

Naiche, L.A., Holder, N., and Lewandoski, M. (2011). FGF4 and FGF8 comprise the wavefront activity that controls somitogenesis. Proc. Natl. Acad. Sci. USA *108*, 4018–4023.

Neijts, R., Simmini, S., Giuliani, F., van Rooijen, C., and Deschamps, J. (2014). Region-specific regulation of posterior axial elongation during vertebrate embryogenesis. Dev. Dyn. *243*, 88–98.

Neijts, R., Amin, S., van Rooijen, C., Tan, S., Creyghton, M.P., de Laat, W., and Deschamps, J. (2016). Polarized regulatory landscape and Wnt responsiveness underlie Hox activation in embryos. Genes Dev. *30*, 1937–1942.

Olivera-Martinez, I., Harada, H., Halley, P.A., and Storey, K.G. (2012). Loss of FGF-dependent mesoderm identity and rise of endogenous retinoid signalling determine cessation of body axis elongation. PLoS Biol. *10*, e1001415.

Rashbass, P., Wilson, V., Rosen, B., and Beddington, R.S. (1994). Alterations in gene expression during mesoderm formation and axial patterning in Brachyury (T) embryos. Int. J. Dev. Biol. *38*, 35–44.

Rivera-Pérez, J.A., and Magnuson, T. (2005). Primitive streak formation in mice is preceded by localized activation of Brachyury and Wnt3. Dev. Biol. *288*, 363–371.

Rivera-Pérez, J.A., and Hadjantonakis, A.K. (2014). The dynamics of morphogenesis in the early mouse embryo. Cold Spring Harb. Perspect. Biol. *7*, a015867.

Stringer, E.J., Duluc, I., Saandi, T., Davidson, I., Bialecka, M., Sato, T., Barker, N., Clevers, H., Pritchard, C.A., Winton, D.J., et al. (2012). Cdx2 determines the fate of postnatal intestinal endoderm. Development *139*, 465–474.

Takada, S., Stark, K.L., Shea, M.J., Vassileva, G., McMahon, J.A., and McMahon, A.P. (1994). Wnt-3a regulates somite and tailbud formation in the mouse embryo. Genes Dev. *8*, 174–189.

Takemoto, T., Uchikawa, M., Yoshida, M., Bell, D.M., Lovell-Badge, R., Papaioannou, V.E., and Kondoh, H. (2011). Tbx6-dependent Sox2 regulation determines neural or mesodermal fate in axial stem cells. Nature *470*, 394–398.

Tsakiridis, A., and Wilson, V. (2015). Assessing the bipotency of in vitro-derived neuromesodermal progenitors. F1000Res. *4*, 100.

Tsakiridis, A., Huang, Y., Blin, G., Skylaki, S., Wymeersch, F., Osorno, R., Economou, C., Karagianni, E., Zhao, S., Lowell, S., and Wilson, V. (2014). Distinct Wnt-driven primitive streak-like populations reflect in vivo lineage precursors. Development *141*, 1209–1221.

Turner, D.A., Hayward, P.C., Baillie-Johnson, P., Rué, P., Broome, R., Faunes, F., and Martinez Arias, A. (2014). Wnt/β-catenin and FGF signalling direct the specification and maintenance of a neuromesodermal axial progenitor in ensembles of mouse embryonic stem cells. Development *141*, 4243–4253.

Tzouanacou, E., Wegener, A., Wymeersch, F.J., Wilson, V., and Nicolas, J.F. (2009). Redefining the progression of lineage segregations during mammalian embryogenesis by clonal analysis. Dev. Cell *17*, 365–376.

van den Akker, E., Forlani, S., Chawengsaksophak, K., de Graaff, W., Beck, F., Meyer, B.I., and Deschamps, J. (2002). Cdx1 and Cdx2 have overlapping functions in anteroposterior patterning and posterior axis elongation. Development *129*, 2181–2193.

van de Ven, C., Bialecka, M., Neijts, R., Young, T., Rowland, J.E., Stringer, E.J., Van Rooijen, C., Meijlink, F., Nóvoa, A., Freund, J.N., et al. (2011). Concerted involvement of Cdx/Hox genes and Wnt signaling in morphogenesis of the caudal neural tube and cloacal derivatives from the posterior growth zone. Development *138*, 3451–3462.

van Rooijen, C., Simmini, S., Bialecka, M., Neijts, R., van de Ven, C., Beck, F., and Deschamps, J. (2012). Evolutionarily conserved requirement of Cdx for post-occipital tissue emergence. Development *139*, 2576–2583.

Visel, A., Minovitsky, S., Dubchak, I., and Pennacchio, L.A. (2007). VISTA Enhancer Browser—a database of tissue-specific human enhancers. Nucleic Acids Res. *35*, D88–D92.

Wilkinson, D.G., Bhatt, S., and Herrmann, B.G. (1990). Expression pattern of the mouse T gene and its role in mesoderm formation. Nature *343*, 657–659.

Wilson, V., and Beddington, R. (1997). Expression of T protein in the primitive streak is necessary and sufficient for posterior mesoderm movement and somite differentiation. Dev. Biol. *192*, 45–58.

Wilson, V., Olivera-Martinez, I., and Storey, K.G. (2009). Stem cells, signals and vertebrate body axis extension. Development *136*, 1591–1604.

Wymeersch, F.J., Huang, Y., Blin, G., Cambray, N., Wilkie, R., Wong, F.C., and Wilson, V. (2016). Position-dependent plasticity of distinct progenitor types in the primitive streak. eLife *5*, e10042.

Yamaguchi, T.P., Bradley, A., McMahon, A.P., and Jones, S. (1999). A Wnt5a pathway underlies outgrowth of multiple structures in the vertebrate embryo. Development *126*, 1211–1223.

Yoshikawa, Y., Fujimori, T., McMahon, A.P., and Takada, S. (1997). Evidence that absence of Wnt-3a signaling promotes neuralization instead of paraxial mesoderm development in the mouse. Dev. Biol. *183*, 234–242.

Young, T., Rowland, J.E., van de Ven, C., Bialecka, M., Novoa, A., Carapuco, M., van Nes, J., de Graaff, W., Duluc, I., Freund, J.N., et al. (2009). Cdx and Hox genes differentially regulate posterior axial growth in mammalian embryos. Dev. Cell *17*, 516–526.

Zaret, K.S., and Mango, S.E. (2016). Pioneer transcription factors, chromatin dynamics, and cell fate control. Curr. Opin. Genet. Dev. *37*, 76–81.

Zhang, Y., Liu, T., Meyer, C.A., Eeckhoute, J., Johnson, D.S., Bernstein, B.E., Nusbaum, C., Myers, R.M., Brown, M., Li, W., and Liu, X.S. (2008). Model-based analysis of ChIP-seq (MACS). Genome Biol. *9*, R137.